FEM analysis of stresses generated in Thermal Barrier Coating with and without intermediate bond coat on Ni-base superalloy substrate

M. Mahesh Kumar[1] , R. Markandeya[2], M S Rawat[3]

[2]JNTU Kukatpally – College of Engineering Kukatpally, Hyderabad, Telangana -500085, INDIA.
[3]MJCET Hyderabad, Muffakam Jah College of Engineering and Technology, Hyderabad – 500 093, INDIA

Abstract: Thermal Barrier Coatings (TBCs) are thin layer of ceramic coating applied on components exposed to higher temperature to enhance the life. Manufacturers design variety of ceramic powders by combining the ceramic constituents. Ceramic powders gets adhered to metal to protect the metal substrate from heat and corrosive gases. Adhesion of powders depends on the thermal and physical properties of coating powder and metal substrate and the coating method employed HVOF, Plasma coating. The stress generated on the coating for due to combined effects of coating and metal substrate is essential for verification on the suitability of the coatings. Analysis of stresses using FEM method helps to predict the nature of stress generated and to predict the coating thickness requirement and help in use of best combination of thickness and method of coating applied. Therefore, simulation techniques such as FEM prove to be worth time saving as they help in reducing time consuming material and experiments as well as give precise results. FEM analysis was done to predict the stresses developed and the effect of intermediate bond coat to minimize the stress developed. These studies will be useful to predict the stresses location on the component and defect formation in TBCs during operation in turbine components.

Keywords: Plastic Stress, Strain; Finite Element Methods;

1. Introduction

Coatings subjected to high-temperature applications experience high thermal stresses and deform plastically during service, leading to spallation, void creation, and complete peel-off coating from the metal substrate. Finding such a phenomenon requires enormous experimental work. A combined effect of thermal and structural problem study is helpful in the prediction of thermal stresses of coatings using the finite element method. The analytical method reduces the number of experimental work and helps predict the behavior of materials under various conditions. The finite element method is used in this work to predict thermal stresses developed in coatings. Results obtained from the FEM method predict the bond coat diffuse in the metal substrate and intactness of bond coat with the metal substrate. The bond coat's intermediate layer, i.e., the intermediate layer of the Top Coat, acts as an initiation site for delamination [1-2].

In FEM, various coating thicknesses 100, 150, 200, 250 and 300 microns were studied to evaluate mechanical stress and strain behavior in X, Y, XY, directions.

The stress evaluation on coating and substrate using FEM analysis indicated that the probable sites for initiating various damage mechanisms are highest at the interface (i.e., towards the unconstrained end). It was also observed that most plastic strain observed in coatings or on the substrate was due to elastic and thermal mismatch on the interfaces and are the most vulnerable sites for damage to start.

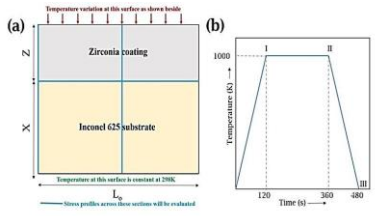

Figure 1.0 Problem statement indicating (a) geometry to be evaluated with ZrO_2 coating on Inconel 625 substrate and boundary conditions, (b) Thermal cycle imposed at the location as mentioned in (a).

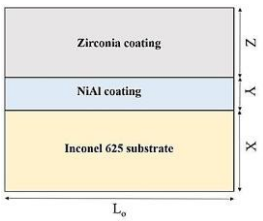

Figure 1.1: Profile and Geometry of TBC coating and substrate along with bond coat layer.

2. Analysis of residual strain in TBCs using Finite Element Methods

2.1 Elements used in FEM:

In FEM we can use two elements for study of thermal-structure problems as shown in Fig.2.1. Plane 13 and Plane 223

elements were taken, as shown in Figure 2.2 (a), (b) respectively; Plane 13 element is chosen for a 2D coupled substantial field element with Ux, Uy, Az (magnetic vector potential), degrees of freedom. Plane 223 is an 8- node 2D coupled substantial field element with Ux, Uy, temp, voltage degrees of freedom. [3-6]

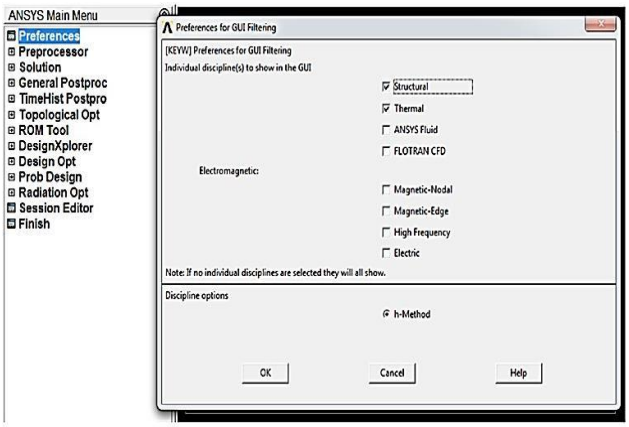

Figure 2.1 thermal structural problem study parameters used

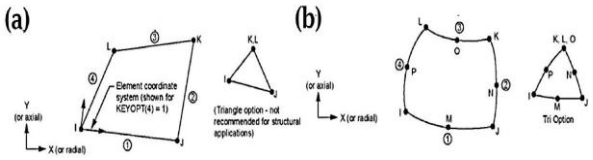

Figure 2.2 Thermal-structural elements (a) Plane 13 (b) Plane 223 current versions

In this work, we have chosen the Plane 223 element as an element.

For thermal structural problems Triangular elements, are not useful. The capabilities of the plane 223 element are as follows:

Structural-thermal analysis
Thermal-piezoelectric
Piezo-resistive
Piezo-electric
Thermal-electric
Electro-elastic
Structural-thermoelectric applications

We limit our work only for Structural Thermal capability. The options chosen for the capatiblities that can form is only chosen in software for structural-thermal, and element behavior is taken as a Plane 223 element from the Coupling Field tab and selected the Quad8node 223 element, and click OK as shown in Fig.2.3 with plane strain.

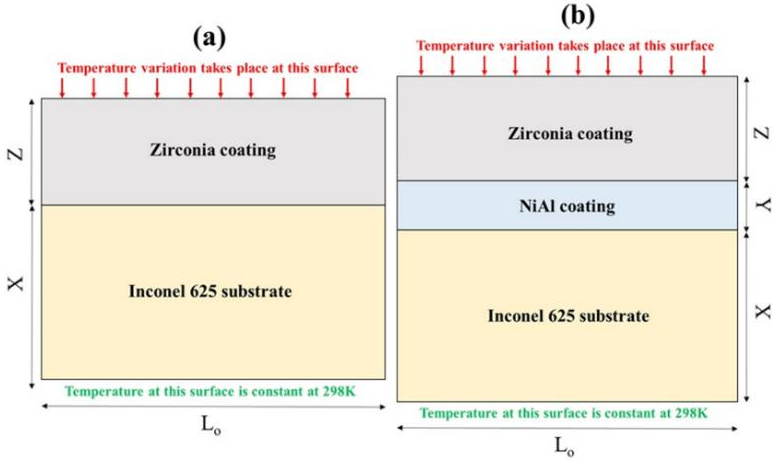

Figure 2.3: (a) Geometry, material and boundary conditions used for FEM analysis in (a) TBC and substrate, (b) TBC, bond coat and substrate

To carry the required thermal-structural analysis, mechanical properties of substrate, bond coat and TBC properties were taken at various temperatures as shown in Table 1 for substrate (Alloy 625) are taken from [7-8]. Also properties of bond coat material (NiAl) taken from [28] and 100% dense ZrO2 (TBC) taken from [9] are tabulated in Tables 2 and 3, respectively. The mechanical properties of the substrate which were not available directly and required for analysis were calculated from [10] by the following equation derived from eq.1.

$$\frac{1}{T} = \frac{1}{H} + \frac{1}{E} \qquad \text{eq. (1).}$$

where T is tangent modulus, H is plastic modulus and E is elastic modulus.

Table 1: Mechanical and thermal properties of Alloy 625

Temperature (K)	294	477	700	922	1033	1144	1366
E (GPa)	207.5	197.9	185.5	170.3	-	147.5	-
$\boldsymbol{\sigma_{ys}}$ **(MPa)**	479.2	-	-	265	244	227	-
ν	0.278	0.286	0.295	0.321		0.336	-
$\boldsymbol{\varepsilon_f^a}$	0.54	-	-	0.72	0.92	1.10	-
$\boldsymbol{\sigma_{UTS}}$ **(MPa)**[a]	965.3	-	-	750	524	265	-
T (MPa)[b]	900	-	-	672.4	304.3	34.59	-
α $(\mathbf{K^{-1}X\ 10^{-6}})$		13.1	13.7	14.8	-	15.8	-
$\mathbf{C_P(J\ Kg^{-1}K^{-1})}$	410	456	511	565	-	620	670
k $(\mathbf{W\ m^{-1}K^{-1}})$	9.8	12.5	15.7	19.0	-	22.8	-
ρ $(\mathbf{kg\ m^{-3}})$	8440	-	-	-	-	-	-

[a] Extracted from [25-27]; [b] Calculated values.

Table 2: Mechanical and thermal properties of NiAl [28]

Temperature (K)	293	773	800	873	1000	1273	1473	1573
E (GPa)	169	155	-	-	-	128	-	81
$\boldsymbol{\sigma_{ys}}$ **(MPa)**	1453	1262	-	-	-	299	-	54
ν	0.32	0.32	-	-	-	0.32	-	0.32
$\boldsymbol{\varepsilon_f}$	0.075	0.02	-	-	-	0.012	-	0.025
α $(\mathbf{K^{-1}X\ 10^{-6}})$	12.91	15.23	-	-	-	17.22	-	17.99
$\mathbf{C_P(J\ Kg^{-1}K^{-1})}$	383	-	640	-	680	-	-	-
k $(\mathbf{W\ m^{-1}K^{-1}})$	87	-	-	78.6	-	-	73.2	-
ρ $(\mathbf{kg\ m^{-3}})$	5900	-	-	-	-	-	-	-

Table 3: Mechanical and thermal properties of 100% dense ZrO_2 [29]

Temperature (K)	293	673	1073	1473
E (GPa)	53	52	46	48
ν	0.25	0.25	0.25	0.25
α $(\mathbf{K^{-1}X\ 10^{-6}})$	7.2	9.4	16	22
$\mathbf{C_P(J\ Kg^{-1}K^{-1})}$	500	576	637	656
k $(\mathbf{W\ m^{-1}K^{-1}})$	1.5	1.2	1.2	1.1
ρ $(\mathbf{kg\ m^{-3}})$	6037	6037	6037	6037

Heat loads are introduced in the form of temperature rise maintaining linear relation with time over the TBC as shown in Fig. 2..3 Step 1 shows heating cycle of the TBC layer from room temperature to 1000 K in 120 s, the TBC at 1000K is held at the same temperature for 240 s in Step 2 and Step 3 involves cooling down of the TBC coated sample from 1000 K back to room temperature

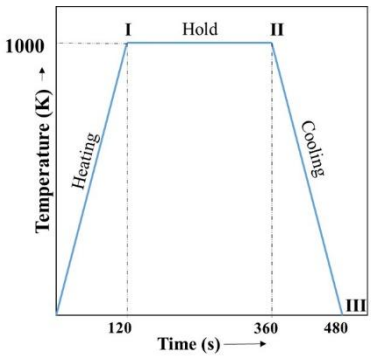

Figure 2.3: Thermal cycle imposed over the TBC coating

FEM analysis in terms of plastic strain obtained after Step 3 for TBC-Substrate and TBC-Bond coat-Substrate combinations are shown in Fig. 2.4(a), 2.4(b), respectively. It helps in predicting that the total mechanical strain order reduced by almost a factor of 10 on application having bond coat layer in between substrate and TBC Coat. Also, it was observed that the plastic strain is located inside the coating, i.e. in between bond-coat and substrate away from the edges. This is in line with other reported studies [7-10]. Hence, the presence of an l bond coat layer helped in reducing plastic strain by an aspect of 10. This is useful in terms of adhesion behavior of the coating to the substrate to have intermediate bond coat. However, this method helped in locating the most probable critical locations inside the coatings when plastic strain is high subsequent to thermal cycling. The locations are the most pone areas in initiating the defects such as delamination, spallation, etc. due to accumulation of plastic strain inside the coating. The values of residual stresses (σxx, σyy and σxy) that developed when thermal cycling is applied in the sample after Step 3 and values found to be in the range of -12.7 MPa to 9.36 MPa in value of magnitude.

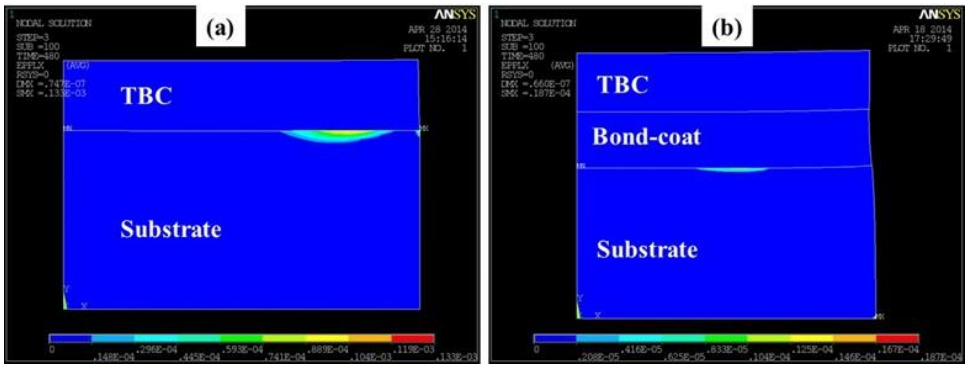

Figure 2.4: Results of plastic strain component after 1 thermal cycle in X direction by using FEM (a) First case of TBC and Substrate e and (b) second case of TBC, in between Bond-coat and Substrate case.

3. Results

3.1 Analysis of Thermal Stresses:

X component of stresses: In steps 1 and 2 (Fig. 3.1), the stress value at the interface was changed from 150-263 MPa in case of 100 µm coating to 16-103 MPa in case of 300 µm coating. Also, the maximum stress acting the interface was increasing. However, the maximum value was observed closer to the unconstrained end than the constrained end. In step 3 (Fig. 4.6), the stresses converted to compressive stress at the interface upon removal of thermal load which indicates tensile property of the material during thermal load. Qualitatively this was valiadated through experiments for bimetallic material thermal mismatch cases.

Y component of stresses: In steps 1 and 2 (Fig. 3.2), the stress value at the interface was changed from (from 11.6-79.2 MPa in case of 100 µm coating to 24.4-89.8 MPa in case of 300 µm coating. But interestingly, with increasing thickness the maximum stresses decreases. However, in case of bond coat presence, the stress value was increased to 30.3-101 MPa, there was minimal stress was present in the ZrO_2 coating.

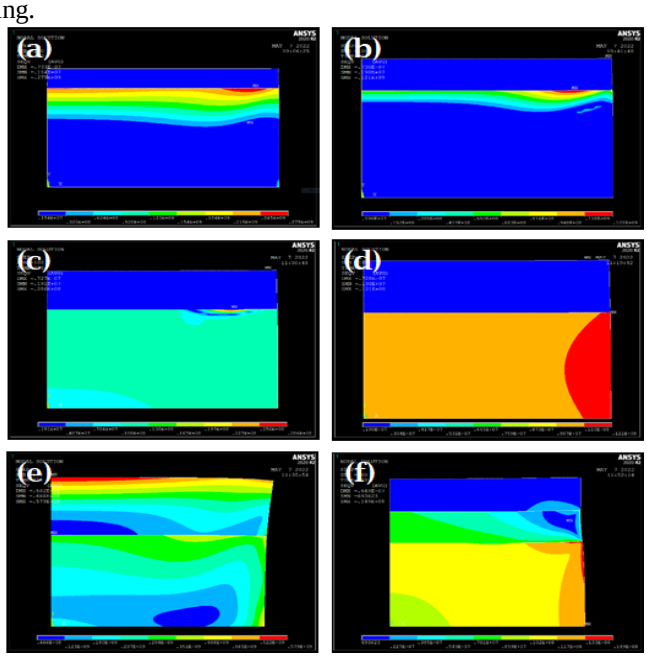

Figure 3.1 Von-Mises equivalent elastic stresses (a) 100 µm ZrO_2 coating (b) 150 µm ZrO_2 coating (c) 200 µm ZrO_2 coating (d) 250 µm ZrO_2 coating (e) 300 µm ZrO_2 coating (f) 200 µm NiAl bond coat and 200µm ZrO_2 coating

3.2 Analysis of Plastic Strain:

Plastic Strain: Plastic strain component plays an important role in understanding delamination of coating. Since due to effect of plastic strain, discontinuity of coating will generate and results in delamination or spallation during operation.

X component of plastic strain: In step 1 and step 2 (Fig.3.1), the resultant maximum strain at the interface in between the unconstrained and constrained portion of interface, the value reduces as coating thickness increases upto 200 mm beyond and it becomes zero (when no plastic strain further available and the strain is present either elastic or thermal only). It was observed that the presence of bond coat is helpful to reduce the plastic strain between the TBC coat and the substrate and in comparison to the non-use of bond coating. Hence, bond coat is extremely beneficial. In step 3 (Fig4.11), same situation exists as plastic deformation is permanent and cannot be reversed upon unloading (either thermally or structurally).

Y component of plastic strain: In step 1 and step 2 as shown in (Fig.3.2) for 100,150 µm coating thickness the maximum strain along the interface from the constrained end, whereas for 200 µm in step 3 as shown in Fig.3.2, bond coat case strain is maximum at the region in between the constrained and unconstrained portions of interface. Similar to x-component, Y-component is also absent in 250,300 µm cases.

.

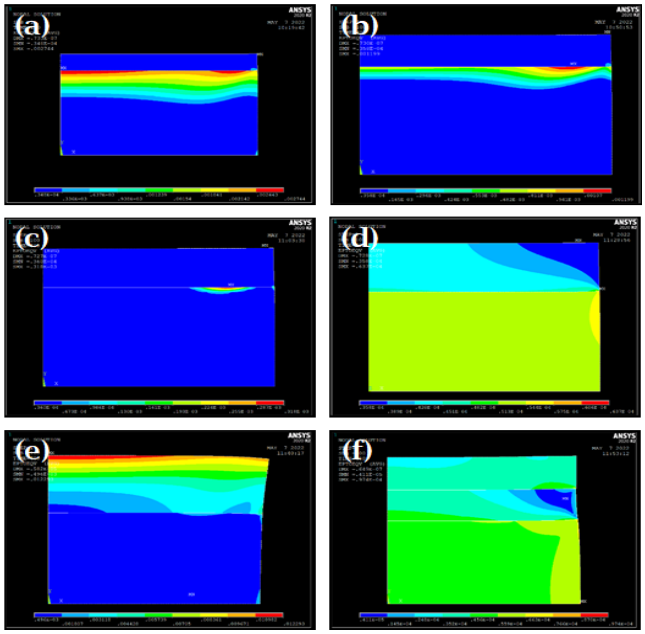

Figure 3.2 Von-Mises mechanical strain Step 3 (a) 100 µm ZrO_2 coating (b) 150 µm ZrO_2 coating (c) 200 µm ZrO_2 coating (d) 250 µm ZrO_2 coating (e) 300 µm ZrO_2 coating (f) 200 µm NiAl bond coat and 200µm ZrO_2 coating

4. Conclusions

From the present study, with reasonable assumptions, FEM results indicated that there is an increase in the plastic strain towards the inside of the coating surface. The stress results obtained are highest at the interface i.e towards the unconstrained end which may acts probable initiation sites and results in damage or delamination by various mechanisms. It was observed that most of the strain observed in coating or substrate was due to elastic and thermal contributions and only at the interface. There was plastic strain, thereby, proving that fact that interfaces are vulnerable sites for damage. Plastic deformation is prominent in 100, 150, 200µm cases while there is no plastic deformation in case of 250,300µm cases. However, when compared for 200µm coating thickness with and without (200µm) bond coat, it was observed that the plastic deformation was reduced by a factor of 10. Hence, FEM proves to be a useful tool to optimize the thickness parameters to eliminate plastic deformation which may lead to problems in case of coating such as spallation, delamination, etc. exposing the pristine material o oxidizing/corroding environments. A slightly thicker coating beyond 200µm with a bond coat would ensure that there is no plastic deformation at the interface and hence, would be fruitful for thermal cycling applications. This procedure for thermal cycling analysis was inexpensive and time saving as compared to the experimental means of observing spallation, etc. behavior. Also, this procedure gives insight into why spallation might take place and critical locations of coatings which can spall off.

Acknowledgements

Authors express their gratitude to the management of BHEL for funding and providing resources for this study.

References

1. GE Modular gas turbine available at: http://www.arabianoilandgas.com/article-9900-ge-saves-qutargas-time-with-modular-turbines-switch/.UzpldpmSxnY
2. science, 12 (2012) pp. 280-284
3. Information provided in ANSYS 13.0 help package
4. Atlas of stress-strain curves, pp.671
5. Inconel 625 datasheet, hot-rolled and annealed sheet data, M/s special metals Inc., USA
6. Journal of materials processing technology, 211 (2011) pp. 1480
7. Journal of materials processing technology, 190 (2007) pp. 29
8. Materials science and engineering A, 277 (2000) pp. 68
9. C. Borri, A. Lavacchi, A. Fossati, I. Perissi, U. Bardi, Proceedings of the COMSOL Conference, Milan, 14 October 2009, 1-7. Available from https://www.comsol.com/paper/download/44874/Borri.pdf
10. M. Schweda, T. Beck, M. Offermann, L. Singheiser, Surf. Coat. Technol. 217 (2013) 124–128. https://doi.org/10.1016/j.surfcoat.2012.12.002.